

## DESIGN OF SOLAR DRYERS FOR SMALL-SCALE FARMERS IN DEVELOPING COUNTRIES

**P. Talbot<sup>1\*</sup>, C. Heilporn<sup>1</sup>, A. Schubert<sup>2</sup>, C. Delannoy<sup>2</sup>, B. Haut<sup>1</sup>**

<sup>1</sup>*Université Libre de Bruxelles, Transfers, Interfaces and Processes (TIPs), Chemical Engineering Unit, av. F.D. Roosevelt 50, CP 165/67, 1050 Brussels, Belgium*

<sup>2</sup>*Université Libre de Bruxelles, Laboratoire d'Anthropologie des Mondes Contemporains (LAMC), Sociology institut, av. Jeanne 44, CP 124, Brussels, Belgium*

*\*Corresponding author: Tel.: +32 2 650 67 57, E-mail: ptalbot@ulb.ac.be*

**Abstract:** The design of a tunnel solar dryer for small-scale farmers in developing countries is presented in this work. A sizing method based on heat and mass balance equations is proposed. This method allows determining the length of a dryer of fixed width, according to the target product to dry, the climatic conditions of the site of drying and the desired drying time. Using this sizing method, a dryer able to dry 10 kg of mangoes in Banlung (Cambodia) was built. Experiments led on this dryer demonstrate that the technology and its sizing method are valid.

**Keywords:** solar dryer, sizing method, drying experiments, mangoes drying

### INTRODUCTION

Solar drying is one of the oldest drying methods used to preserve food. In hot countries, most farmers dry their harvest directly in the sun by spreading the products on the floor. This method often leads to production losses and to a degradation of the products quality. Indeed, the products are directly subject to the sun UVs, to many contaminations such as dust, insects, fungi, birds, and to bad weather. Moreover, drying on the ground is a time consuming operation.

To overcome these difficulties, several authors developed efficient solar dryers in which the products are protected from environmental constraints.<sup>[1,2,3]</sup> The types of dryers are numerous according to the product to dry, its quantity and the technology chosen.<sup>[3]</sup> Some dryers are partially or completely dependent of the sun energy. They work with or without ventilation. The product can be directly heated by the sun radiations or dries in contact with air previously heated by the sun radiations. Both ways to bring energy to the product can also be combined. The problems often met in the implementation of these dryers is that local communities are not involved enough in the projects and/or the lack of design methodology.

In this work, solar dryers are designed with energy and mass balance equations for small-scale farmers in developing countries. The technology selected is a ventilated tunnel solar dryer in which the product is

protected from external contaminations and gets energy from previously heated air combined with direct sun radiations. Within the context of the European FP7 project, Annâdya, a dryer sized to process 10kg of fresh mangoes a day in Banlung (Cambodia) was build and tested on the field.

### DESCRIPTION OF THE TECHNOLOGY

A schematic diagram of the tunnel solar dryer is shown in Fig. 1. The air flows through the dryer thanks to fans (1) supplied with a photovoltaic solar panel (2). These fans are included in a slab to keep the tunnel hermetic to wind, dust or insects. A transparent plastic covers the whole tunnel and creates a greenhouse effect inside. Sun direct and diffuse radiations go through the plastic layer and are captured by a black flat floor placed along the dryer. The heat exchanges taking place into the tunnel dryer are described in more details in the next section: sizing method. The length of the dryer is divided in two parts. The heating part (3) is product free and is used to heat the air passing through it to a target drying temperature. The heated air then enters the drying part (4). The products are placed in this part on a net slightly raised from the floor. The goal is to keep the air temperature in the drying part constant on a drying time average. Therefore, the dimensions of this part have to be chosen in a way that the energy necessary to evaporate products water is offset by the energy brought by the sun radiations. The air humidity increases along the drying part. Finally, the humidity is evacuated at the end of the

tunnel dryer. Except for this exit, the airtightness of the tunnel dryer is of high importance.

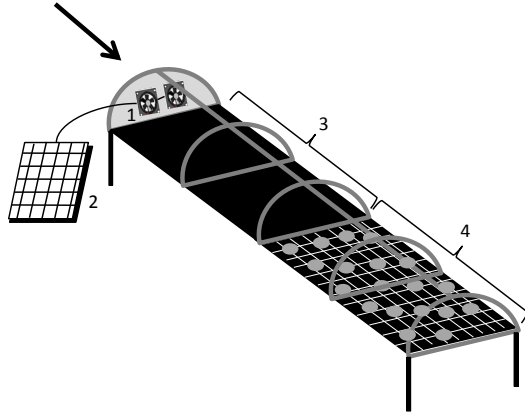


Fig. 1. Schematic diagram of a solar dryer

### SIZING METHOD

A sizing method of the tunnel solar dryer mainly based on energy and mass balance equations is established with the software Mathematica 7<sup>®</sup>. This sizing method allows determining the lengths of the two parts of a dryer of fixed width, according to the quantity of the product to dry, its initial and desired final humidities and its ideal drying temperature but also according to the climatic conditions of the site of drying and the desired drying time. Moreover, it includes the sizing of the ventilation system.

The different heat fluxes taken into account in the solar dryer sizing are represented on transversal cuts of the heating and the drying parts in Fig. 2 a and b, respectively.

In the heating part, the black flat floor heats by capturing direct and diffuse solar radiations,  $F_D$ . The top of the plastic layer captures infrared radiations from the atmosphere,  $F_{amb}$ . Inside the tunnel, infrared radiations are exchanged between the black floor and the bottom part of the plastic,  $F_{fl-p,i}$ . Infrared radiations are lost by the top of the plastic into the atmosphere,  $F_{p,e}$ . The second heat loss occurs by convection at the external surface of the plastic,  $F_{conv,p,e}$ . Heat conduction takes place in the thickness of the plastic,  $F_{cond,p}$ . Finally, the air passing through the heating part heats by convective heat transfers with the black floor,  $F_{conv,fl}$ , and with the plastic,  $F_{conv,p,i}$ .

In the drying part, the heat fluxes are similar to those of the heating part excepted on the floor. Indeed, an additional heat transfer appears due to an evaporation term,  $EV$ . This term represents the heat necessary to evaporate the water of the product averaged on the drying time.

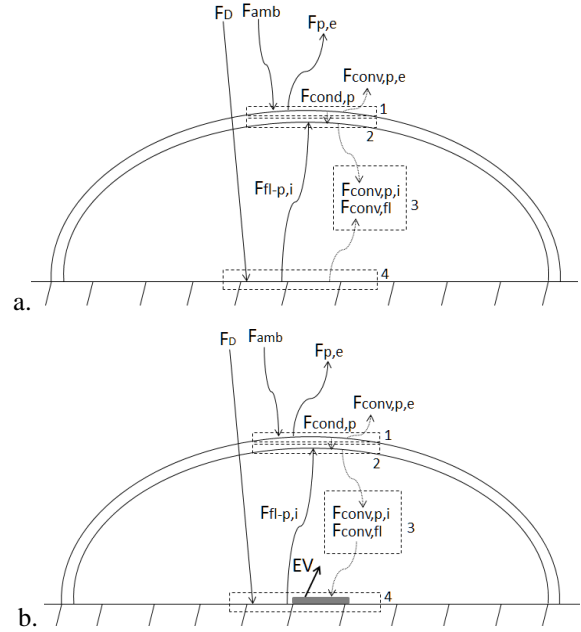


Fig. 2. Heat fluxes (W/m<sup>2</sup>) represented in a transversal cut of the heating part (a) and the drying part (b) of the tunnel solar dryer.

The heat transfers balances expressed on the four grey boxes of the Fig. 2 are described by the system of Eq. 1, 2, 3 and 4a for the heating part and by the system of Eq. 1, 2, 3 and 4b for the drying part. Equations numbers correspond to box numberings. The resolution of these four equations including five unknowns ( $T_{p,e}$ ,  $T_{p,i}$ ,  $T_{fl}$ ,  $T_{air}$  and  $P(t)$ ) allows to express  $P(t)$ , the heat flux transferred to the air in the dryer, as a function of the time, via  $F_D(t)$ , and the temperature of the entering air,  $T_{air}$ . To evaluate the air temperature after a given distance inside the tunnel, the dryer is divided in length in zones of length  $\Delta z$ . Eq. 5 is used to calculate the air temperature at the end of a zone giving the time and the temperature at the entrance of this zone. Starting with the ambient temperature, it is possible to iteratively obtain the temperature reached after a given number of zones,  $n$ . The length of the heating zone is then determined by trials and errors on the number of zones,  $n$ , until reaching a target drying temperature at the end of the heating part on drying time average. In the same way, the length of the drying zone is determined to get  $P(t)=0$  on drying time average. This means that the energy absorbed by the evaporation is on average compensated by the solar energy that still heats the air passing through the drying part.

$$F_{amb} R = \sigma T_{p,e}^4 R + \frac{\lambda_p}{e_p} (T_{p,e} - T_{p,i}) R + h_{p,e} (T_{p,e} - T_{amb}) R \quad (1)$$

$$\sigma (T_{fl}^4 - T_{p,i}^4) + \frac{\lambda_p}{e_p} (T_{p,e} - T_{p,i}) R = h_{p,i} (T_{p,i} - T_{air}) R \quad (2)$$

$$P(t) = h_{cf}(T_{\beta} - T_{air}) + h_{cf}(T_{p,i} - T_{air})R \quad (3)$$

$$\left\{ \begin{array}{l} F_D(t) S = \sigma(T_{\beta}^4 - T_{p,i}^4) + h_{cf}(T_{\beta} - T_{air}) \\ F_D(t) V = \sigma(T_{\beta}^4 - T_{p,i}^4) + h_{cf}(T_{\beta} - T_{air}) \\ \quad + \frac{D}{(1 + X_0)} \frac{(X_0 - X_f)}{t_d} Lk \end{array} \right. \quad (4a)$$

$$\left\{ \begin{array}{l} F_D(t) V = \sigma(T_{\beta}^4 - T_{p,i}^4) + h_{cf}(T_{\beta} - T_{air}) \\ \quad + \frac{D}{(1 + X_0)} \frac{(X_0 - X_f)}{t_d} Lk \end{array} \right. \quad (4b)$$

$$T_{air,i} = T_{air,i-1} + \frac{P(T_{air,i-1}, t) B \Delta z}{Q C}; i = 0, \dots, n \quad (5)$$

The sizing method requires simulating the solar radiations during the day at the drying place. Direct and diffuse radiations flux,  $F_D$ , is computed as a sinusoidal function from the sunset and sundown times and from the mean radiation flux acquired via FAOClim<sup>[4]</sup>. The ambient infrared flux,  $F_{amb}$ , is estimated from the mean ambient temperature by way of the dew and the sky temperature.<sup>[5]</sup> All climatic data can be found with FAOClim<sup>[4]</sup> or can be deduced from previous years data, if available.

The flow rate that has to be supplied is a very important parameter of the sizing method. The desired flow rate is computed to ensure that the air inside the dryer is never saturated in water on drying time average considering the total water to evaporate. Eq. 6 expresses the air flow ten times higher than the air flow that would saturate the drying air.

$$Q_s = 10 \frac{M}{1 + X_0} (X_0 - X_f) \frac{1}{t_d} \frac{1}{Y_{sat}(T_d) - Y_{amb}} \quad (6)$$

The photovoltaic panel and the fans are chosen in the way that they can deliver the flow rate,  $Q_s$ , on drying time average knowing the solar radiations at the drying place.

#### IMPLEMENTATION OF A TUNNEL SOLAR DRYER IN CAMBODIA

Within the context of the European FP7 project, Annâdya, a dryer sized to process 10 kg of fresh mangoes in 6.5 hours in March in Banlung (Cambodia) was built and tested on the field. The initial humidity of the mangoes are estimated at 7 kg of water per kg of dried matter and the target final humidity is fixed to 0.1 kg of water per kg of dried matter. The total water mass to evaporate is then 7.84 kg. The width of the tunnel is chosen as 1.4 m and the air flow rate is computed as 0.025 kg of air per second. All the data used to size the dryer are presented in Table 1. The convective heat transfer coefficient between the air and the surfaces inside the dryer,  $h_{p,i}$ , is determined with a correlation of mixed convection.<sup>[6]</sup> The convective heat transfer coefficient between the ambient air and the top of the plastic,  $h_{p,e}$ , is determined with the Hilpert correlation considering a slight wind perpendicular to the dryer.<sup>[6]</sup>

The sizing method fixes the length of the heating part to 5 m in order to reach 65°C at the entrance of the drying part on average. The length of the drying part is fixed at 3.6 m by the sizing model. It is finally chosen at 5 m to include a safety factor and eventually dry more mangoes or other types of product. A picture of the dryer built in Banlung is shown in Fig. 3.

Table 1. Values used in the sizing method for the sizing of the Banlung's dryer

Symbol	Value	Units
$B$	1.4	m
$C$	1009	J kg <sup>-1</sup> K <sup>-1</sup>
$D$	5	kg m <sup>-2</sup>
$e_p$	0.001	M
$h_{p,e}$	0.5	W m <sup>-2</sup> K <sup>-1</sup>
$h_{p,i}$	2.4	W m <sup>-2</sup> K <sup>-1</sup>
$Lk$	2358 10 <sup>3</sup>	J kg <sup>-1</sup>
$M$	10	kg
$Q_s$	0.025	kg <sub>air</sub> s <sup>-1</sup>
$R$	1.25	-
$S$	0.9	-
$t_d$	6.5	h
$T_{amb}$	31	°C
$T_d$	65	°C
$V$	0.8	-
$X_0$	7	kg <sub>water</sub> kg <sub>dry matter</sub> <sup>-1</sup>
$X_f$	0.1	kg <sub>water</sub> kg <sub>dry matter</sub> <sup>-1</sup>
$Y_{amb}$	0.012	kg <sub>water</sub> kg <sub>dry air</sub> <sup>-1</sup>
$\Delta z$	0.1	m
$\lambda_p$	0.2	W m <sup>-1</sup> K <sup>-1</sup>
$\sigma$	5.67 10 <sup>-8</sup>	W m <sup>-2</sup> K <sup>-4</sup>

The tunnel dryer materials include new and recycle supplies, all available locally. The tunnel is built at around 1.2 m from the floor thanks to a wood construction to avoid dust and facilitate product manipulation. At the entrance of the dryer, two computer fans (12V, DC) were included in a plywood slab. The floor of the tunnel is made of three layers. Plywood slabs, insuring the airtightness of the tunnel bottom, is covered by an insulating polystyrene layer made of used ice boxes pieces. Black textile is placed over the polystyrene layer. The semi-circular structure is made of bamboo stalks. The covering plastic layer is attached at the wood structure with binder clips in a way to insure airtightness. In the drying part, a large horizontal net is built with string fixed at the bamboo stalks at around 15 cm of the dryer floor. The product is

spread on a mosquito net placed directly on the string net. The width of the product surface is 1.2 m.



Fig. 3. Tunnel solar dryer built in Banlung.

### INSTRUMENTATION AND EXPERIMENTS

Three experiments of mangoes drying (M1, M2 and M3) were monitored with air temperatures and humidity along the dryer. The ambient temperature,  $T_{amb}$ , was measured outside of the entrance dryer, in the shadow and sheltered from the wind with a Testo® 905-T1 thermometer. The temperature at the end of the heating part,  $T_{mid}$ , was monitored with a CheckTemp1 by Hanna Instruments®. The ambient air humidity,  $Y_{amb}$ , was measured with a digital thermometer-hygrometer by TFA®. The air temperature and humidity at the end of the mangoes zone,  $T_{out}$  and  $Y_{out}$ , were monitored with a Hobo® data logger Temp/HR U12-011. Direct and diffuse solar radiations were measured with a solarimeter KIMO® SL-100. The air flow in the dryer,  $Q$ , is determined by measuring the air velocity with a Pocket anemometer Xplorer2 by Skywatch®. All data were collected every 20 minutes during drying experiments. Information on each experiment are presented in Table 2.

Table 2. Information on mangoes drying experiments.

	M1	M2	M3
Day (March 2014)	13th	19th	20th
Weather conditions	Sunny all day	Cloudy and windy in the morning	Cloudy and windy in the morning
Fresh mass (kg)	9.8	8.2	11.0
Length occupied (m)	3.65	4.9	5.05
Fresh surface mass ( $\text{kg m}^{-2}$ )	2.24	1.39	1.82
Drying time (h)	6.3	5.75	5.9
Water evaporated (kg)	7.9	6.4	8.5

### RESULTS AND DISCUSSION

Details on the experiments gathered in Table 2 show that the objective of evaporating around 7.8 kg of water from around 10 kg of fresh mangoes is reached. An experimental difference with the sizing method hypotheses is the surface occupied by 1 kg of mangoes. The dryer was sized considering a maximal surface mass of  $5 \text{ kg m}^{-2}$  while the maximal surface mass reached on the field was  $2.24 \text{ kg m}^{-2}$ . As the drying part was built longer than the length predicted by the sizing method, we were able to spread 10 kg of fresh mangoes anyway.

The temperature results monitored during mangoes drying experiments M1, M2 and M3 are presented in Fig. 4 a, b and c, respectively. The cross markers are the ambient temperatures. The circle markers are the temperatures measured at the end of the heating part (filled circles) and at the end of the mangoes zone (empty circles). The experimental results are compared to the temperatures obtained with the sizing method. To obtain these data, the sizing method is used with the diffuse and direct solar flux, the ambient temperatures, the air flows, the product surface mass and the water evaporated mass measured the same day. The temperatures predicted by the sizing method are represented with filled squares for the temperatures at the end of the heating part and with empty squares for the temperatures at the end of the zone with mangoes.

During the experiment M1, the whole day was sunny without clouds and wind. The ambient temperatures vary between  $31.8 \text{ }^\circ\text{C}$  and  $37.5 \text{ }^\circ\text{C}$ . The mean temperature reached at the end of the heating part is  $58.3 \text{ }^\circ\text{C}$ . The highest difference between measured and predicted temperatures is  $3.8 \text{ }^\circ\text{C}$  and the mean absolute difference is  $1.7 \text{ }^\circ\text{C}$ . The mean temperature reached at the end of the zone with mangoes is  $62.9 \text{ }^\circ\text{C}$ .

The morning of experiment M2 was cloudy. The afternoon was sunny. Wind was intermittently blowing during all day. Ambient temperatures during the experiment vary between  $30.9$  and  $37.4 \text{ }^\circ\text{C}$ . The mean temperature reached at the end of the heating part is  $54.8 \text{ }^\circ\text{C}$ . The highest difference between measured and predicted temperatures is  $7.2 \text{ }^\circ\text{C}$  and the mean absolute difference is  $2.1 \text{ }^\circ\text{C}$ . The mean temperature reached at the end of the zone containing mangoes is  $59.4 \text{ }^\circ\text{C}$ .

The slightly windy morning of experiment M3 was followed by a sunny afternoon. An intermittent wind was weak. Ambient temperatures vary between  $30.2$  and  $38.7 \text{ }^\circ\text{C}$  during the experiment. The mean temperature of  $56.7 \text{ }^\circ\text{C}$  is reached at the end of the heating part. The highest difference between measured and predicted temperatures is  $6.1 \text{ }^\circ\text{C}$  and the mean absolute difference is  $1.8 \text{ }^\circ\text{C}$ . The difference of  $6.1 \text{ }^\circ\text{C}$  occurred at 11h10. Just before this measurement, a gust of wind took place,

lowering the dryer temperatures. The mean temperature reached at the end of the mangoes zone is 53.3 °C.

The mean temperatures reached at the end of the heating zone for the three experiments M1, M2 and M3 are lower than the target temperature of 65 °C. This is mainly because the air flows in the dryer measured during the experiments are higher than the air flow used in the sizing method. Indeed, only one type of fans was available in Banlung and two fans were necessary to have a homogeneous drying in the dryer width. The sizing of the ventilation system could not be exactly applied.

With a mean difference of 1.9 °C for the three experiments, the sizing method considering the real drying conditions gives good predictions of the temperatures at the end of the heating parts. Only three predicted temperatures are different of more than 5 °C from experimental data. These experimental data are related to windy conditions. Sheltering the dryer from the wind is then very important.

Generally the mean temperature at the end of the mangoes zone is similar to the mean temperature reached at the end of the heating zone, as the dryer was sized for. The differences are mainly due to the fact that the experimental surface mass of the product is lower than the one used to size the dryer.

For temperatures at the end of the mangoes zone, differences between experimental and predicted temperatures are important, especially in the beginning and at the end of the drying. This is explained by the fact that the sizing method does not take into account the real evaporation kinetics of the product but the mean evaporation rate on drying time average. The evaporation rate being faster at the beginning of the experiment, experimental temperatures are lower at this moment. The opposite situation occurs at the end of the drying, when the evaporation rate lowers, resulting in experimental temperatures higher than the predicted temperatures. This phenomenon is particularly visible at the beginning of the experiment M3. The high fresh mass of this experiment induces a high evaporation rate at the beginning of the experiment, leading to a high temperature difference between experimental and predicted temperatures at the end of the mangoes zone.

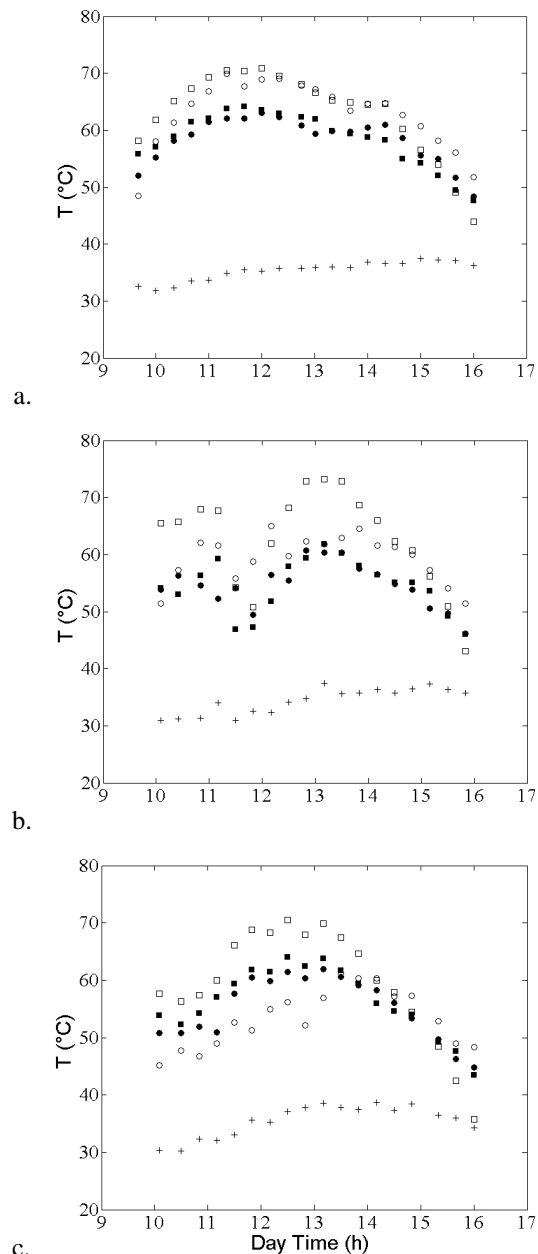


Fig. 4. Day evolution of the temperatures during mangoes drying experiments M1 (a.), M2 (b.) and M3 (c.) with measured ambient temperatures (+) , measured and predicted temperatures at the end of the heating part, (●) and (■), and measured and predicted temperatures at the end of the zone with mangoes, (○) and (□).

## CONCLUSIONS

A tunnel solar dryer designed for small-scale farmers in developing countries is presented in this work. The technology consists in a ventilated tunnel with a black floor and a plastic top in which a greenhouse effect takes place. The air passing through this tunnel is heated in the first part of the tunnel that is product free. The heated air enters next the second part of the dryer where the product to dry is spread.

A sizing method of this technology of solar dryers is developed based on heat and mass balance equations. This sizing method allows determining the lengths of the two parts of a dryer of fixed width, according to the quantity of the product to dry, its initial and desired final humidities and its ideal drying temperature but also according to the climatic conditions of the site of drying and the desired drying time. The lengths are determined in a way that the target drying temperature is reached at the end of the heating part and that the temperature along the drying part is constant on drying time average. Within the context of the European FP7 project, Annâdya, a dryer sized by the developed method to process 10 kg of fresh mangoes in 6.5 hours in March in Banlung (Cambodia) was built. Experimental results obtained with this dryer show that the design is performant. Indeed, target temperatures are reached at the end of the heating zone, temperatures at the entrance and at the exit of the drying part are similar and the mangoes are dried at the end of the drying time. Furthermore the comparison of experimental temperatures with the temperatures predicted by the sizing method show that the equations proposed are a good representation of the real transfer phenomena. Moreover, the dryer was built with local people in Banlung so that knowledge is transferred.

#### NOMENCLATURE

B	dryer width	m
C	heat capacity	$\text{Jkg}^{-1}\text{K}^{-1}$
D	surface mass of the fresh product	$\text{kg m}^{-2}$
e	thickness	m
F	solar flux	$\text{Wm}^{-2}$
h	convective heat transfer coefficient	$\text{Wm}^{-2}\text{K}^{-1}$
L	length of the heating/drying part	m
Lk	water latent evaporation heat	$\text{J kg}^{-1}$
M	fresh mass	$\text{kg m}^{-2}$
n	length divisions number	-
P	heat flux transferred to air inside the dryer	$\text{Wm}^{-2}$
Q	air flow in the dryer	$\text{kg h}^{-1}$
R	ratio of lengths between the floor and the curved plastic top widths	-
S	shadow factor in the heating part	-
t	time	s
T	temperature	K
V	shadow factor in the drying part	-
X	product humidity	$\text{kg}_{\text{water}}$ $\text{kg}_{\text{dry},1}$ matter
Y	air humidity	$\text{kg}_{\text{water}}^{-1}$ $\text{kg}_{\text{dry air}}$

#### Greek letters

$\lambda$	thermal conductivity	$\text{Wm}^{-1}\text{K}^{-1}$
$\sigma$	Stefan-Boltzmann constant	$\text{Wm}^{-2}\text{K}^{-4}$

#### Subscripts

0	initial
air	air inside the dryer
amb	ambient
cond	conduction
conv	convection
d	drying
D	direct and diffuse
e	external
f	final
fl	dryer floor
i	internal
j	iterative subscript
mid	at the end of the heating part
out	at the end of the mangoes zone
p	plastic
s	sizing
sat	saturation

#### ACKNOWLEDGEMENTS

The authors want to acknowledge the F.R.S.-FNRS Fonds de la Recherche Scientifique for their financial support.

#### REFERENCES

- Sharma, A.; Chen, C.R.; Vu Lan, N. Solar energy drying systems: A review. *Renewable and Sustainable Energy Reviews* **2009**, 13, 1185–1210.
- Fudholi, A.; Sopian, K.; Ruslan, M.H.; Alghoul, M.A.; Sulaiman, M.Y. Review of solar dryers for agricultural and marine products. *Renewable and Sustainable Energy Reviews* **2010**, 14, 1–30.
- VijayaVenkataRaman, S.; Iniyar, S.; Goic, R. A review of solar drying technologies. *Renewable and Sustainable Energy Reviews* **2012**, 16, 2652–2670.
- FAOclim software  
<http://faoclim.software.informer.com/2.0/>  
Downloaded the 9<sup>th</sup> of May 2012.
- Lienhard IV, J.H.; Lienhard V, J.H. *A Heat Transfer Textbook*; Phlogiston Press: Cambridge, 2004.
- Becker, M. *Heat Transfer: A Modern Approach*; Springer New York, 1986.